

A bioorthogonal  $^{68}\text{Ga}$ -labelling strategy for rapid *in vivo* imaging†

Cite this: *Chem. Commun.*, 2014, 50, 9557

Received 21st May 2014,  
Accepted 4th July 2014

DOI: 10.1039/c4cc03903c

www.rsc.org/chemcomm

Herein, we describe a fast and robust method for achieving  $^{68}\text{Ga}$ -labelling of the EGFR-selective monoclonal antibody (mAb) Cetuximab using the bioorthogonal Inverse-electron-Demand Diels–Alder (IeDDA) reaction. The *in vivo* imaging of EGFR is demonstrated, as well as the translation of the method within a two-step pretargeting strategy.

Bioorthogonal chemical reactions are closely associated with the characteristics of ‘click’ chemistry, occurring with high selectivity and fast reaction kinetics *in vivo*.<sup>1,2</sup> More specifically, these reactions occur under physiological conditions, without interfering with any of the native biological processes to which they may be exposed. Key bioorthogonal reactions include the Staudinger–Bertozzi ligation and Bertozzi’s Strain-Promoted, ‘copper-free’ Azide–Alkyne [3+2] Cycloaddition (SPAAC).<sup>2–4</sup> These reactions are highly robust methods, notably for achieving labelling of cell-surface macromolecules, but their sub-optimal reaction kinetics limit their use in applications requiring low reagent concentrations.<sup>5</sup> The Inverse-electron-Demand Diels–Alder (IeDDA) reaction between tetrazines and strained alkenes was introduced by Fox and co-workers in 2008 as a new bioorthogonal ligation reaction, which displays rates of reaction up to 5 orders of magnitude higher than those demonstrated by the SPAAC reaction, and up to 7 orders of magnitude higher than the Staudinger–Bertozzi ligation.<sup>6–9</sup> A series of  $^{68}\text{Ga}$ -labelled IeDDA reactions were recently validated in our laboratory, whereby the reaction between a  $^{68}\text{Ga}$ -labelled tetrazine and a series of norbornene analogues could be demonstrated in impressive radiochemical conversions at physiological temperatures in aqueous media.<sup>10</sup> Improved reaction kinetics were expected

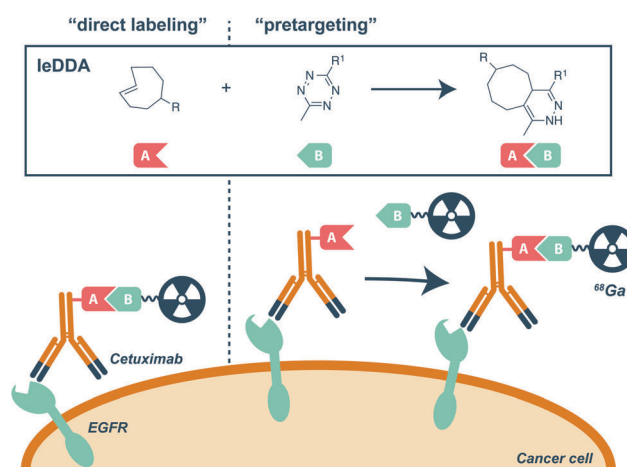


Fig. 1 Schematic illustration depicting the “direct” and “pretargeting” labelling strategies for the non-invasive detection of EGFR expression on cancer cells, using  $^{68}\text{Ga}$ -labelled Cetuximab via IeDDA bioorthogonal ligation.

to be displayed by the more strained *trans*-cyclooctene (TCO) dienophile, and this motivated us to develop a fast and robust labelling procedure for *in vivo* Positron Emission Tomography (PET) imaging of cell surface macromolecules, using the IeDDA reaction between a TCO-modified monoclonal antibody (mAb) and a  $^{68}\text{Ga}$ -labelled tetrazine (Fig. 1).

The development of a fast and efficient method for radio-labelling clinically relevant mAbs remains subject of intense investigation.<sup>11</sup> Cetuximab (C225, Erbitux), a chimeric human/murine IgG1 mAb, which targets the epidermal growth factor receptor (EGFR/ErbB1), was approved by the FDA (Food and Drug Administration) in 2004, and is indicated for the treatment of colorectal and head and neck cancer patients.<sup>12</sup> Subsequently, the development of PET imaging agents that specifically target EGFR became an area of intensive research, with the ultimate goal of enabling stratification of patients and their follow-up treatment. Existing Cetuximab radiolabelling methods, primarily using bifunctional chelators in combination with metal radio-isotopes such as  $^{64}\text{Cu}$  and  $^{89}\text{Zr}$  (half-lives of 12.7 h and 78.4 h,

<sup>a</sup> Comprehensive Cancer Imaging Centre, Department of Surgery & Cancer, Imperial College London, Hammersmith Hospital, London W12 0NN, UK. E-mail: e.aboagye@imperial.ac.uk

<sup>b</sup> Department of Chemistry, Imperial College London, South Kensington Campus, London SW7 2AZ, UK

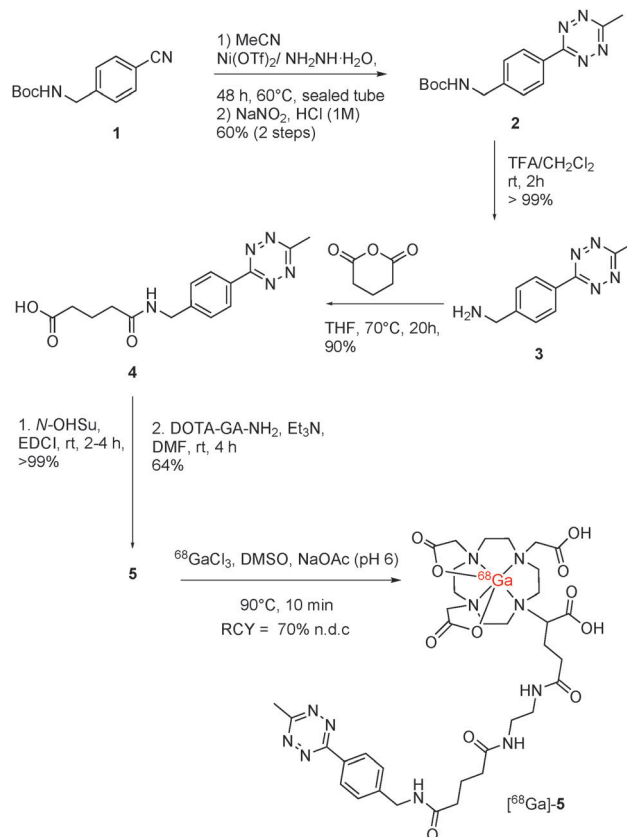
† Electronic supplementary information (ESI) available: Experimental procedures and characterization, radiochemistry methods, additional chemistry and biology supporting figures. See DOI: 10.1039/c4cc03903c

respectively), usually require the use of elevated temperatures and/or long synthesis times, and neither of these factors is readily compatible with the use of mAbs in combination with short-lived PET isotopes.<sup>13–16</sup> Whilst relative successes using <sup>64</sup>Cu- or <sup>89</sup>Zr-labelled Cetuximab have been demonstrated, significant drawbacks, including prolonged radioactive dose to the patient, mixed decay emission and the requirement for a cyclotron facility, could prevent their widespread use in clinical applications.

<sup>68</sup>Ga is rapidly emerging as an attractive radionuclide for PET imaging applications. Its production is achieved using relatively low-cost generators containing the parent nuclide <sup>68</sup>Ge, allowing clinical studies to be carried out without requiring an on-site cyclotron. The isotope is also incorporated *via* relatively simple radiolabelling methods utilizing bifunctional chelates. <sup>68</sup>Ga has, however, not yet been used in the context of antibody labelling, in part due to its relatively short half-life of 68.3 minutes. Moreover, chemistry protocols to incorporate <sup>68</sup>Ga usually require both acidic conditions and heating to at least 80 °C. Herein, we describe a fast and robust method for achieving <sup>68</sup>Ga-labelling of the EGFR-selective Cetuximab mAb using the bioorthogonal IeDDA reaction, and the subsequent non-invasive imaging of EGFR *in vivo*. Moreover, experiments are presented in which a two-step *in vivo* pretargeting method is applied, highlighting the potential utility and versatility of this labelling strategy for the annotation of cell surface markers of cancer with immunoPET.

Tetrazine **3**, containing a methyl substituent in the C-3 position was synthesized for our proposed application, with the aim to obtain an optimal balance between ease of synthesis, thermal stability and reactivity in the IeDDA reaction (Scheme 1).

The structure of our <sup>68</sup>Ga-labelled tetrazine [<sup>68</sup>Ga]-**5** was designed to incorporate a spacer unit between the sterically demanding macrocycle and the reactive tetrazine functional group, in order to enable rapid reaction with TCO-modified proteins. Tetrazine **3** was synthesized *via* a modification of Devaraj's one-pot metal-catalysed method.<sup>17,18</sup> Following deprotection of tetrazine **2**, an acid moiety was introduced onto the synthesized amine **3**, to create a suitable point of attachment to the DOTA-chelate. The resulting carboxylic acid **4** was functionalized with a succinimide ester moiety, and was subsequently coupled with the free amine residue on DOTA-GA-NH<sub>2</sub>, forming conjugate **5** in an overall yield of 34% over 5 steps. The radiosynthesis of our <sup>68</sup>Ga-labelled tetrazine [<sup>68</sup>Ga]-**5** was achieved in just 10 min at 90 °C, and starting with 185 MBq of <sup>68</sup>GaCl<sub>3</sub>, the product was obtained in up to 75% radiochemical yields, end-of-synthesis (n.d.c.), with a specific activity of 40–55 GBq μmol<sup>-1</sup>. The labelling was attempted at pH's ranging from 3.0 to 6.0, and pH 6.0 allowed for the highest conversions to the product, with the lower pH buffers (in the range 3.0 to 5.0) resulting in a larger amount of non-chelated <sup>68</sup>GaCl<sub>3</sub>. Encouragingly, [<sup>68</sup>Ga]-**5** was found to be stable when incubated in PBS at 40 °C over a period of 2 h, showing 100% of the parent species by radio-HPLC (*n* = 3). Evaluation of its *in vivo* biodistribution also indicated rapid urinary clearance from the body (Fig. S4, ESI†). The log *P* was measured to be -2.3, suggestive of a reasonable, but not optimal pharmacokinetic profile for [<sup>68</sup>Ga]-**5**, in the context of prospective application of this approach *in vivo*.



Scheme 1 Synthesis of DOTA-GA-tetrazine **5** from nitrile **1**, and subsequent radiosynthesis of [<sup>68</sup>Ga]-**5**.

The modification of Cetuximab **6** was achieved by incubating the protein with TCO succinimide ester.<sup>9,19</sup> A PEG-4 moiety was used so that a linker between the mAb and the TCO functional group would be introduced, with the hypothesis that this would increase the availability of the dienophile for reaction with tetrazine [<sup>68</sup>Ga]-**5**. 100 molar equivalents of the succinimide were used for the ligation reaction, which was carried out at 4 °C for 16 h. Purification of the protein was carried out using centrifugal filtration, and subsequently confirmed using size-exclusion chromatography (SEC). The resulting modified mAb **7** was characterised by MALDI mass spectrometry, which revealed that an average of 17 TCO moieties had been added to each molecule of Cetuximab (Fig. S1, ESI†). It was confirmed that Cetuximab derivative **7** retained immunoreactivity at levels comparable to the parent mAb **6**, as shown by the inhibition of EGF-induced EGFR phosphorylation in A431 human epidermoid carcinoma cells (Fig. S2, ESI†). The IeDDA reaction between the two reactive species Cetuximab derivative **7** and the conjugate [<sup>68</sup>Ga]-**5** was assessed in PBS up to a time-point of 30 min, and the overall synthesis of [<sup>68</sup>Ga]-**8** could be achieved within 45 min of <sup>68</sup>GaCl<sub>3</sub> elution, giving 75%, 87%, and 95% conversion spontaneously, after "0" min, 15 min and 30 min incubation, respectively (Fig. 2 and Fig. S3, ESI†).

Subsequent *in vivo* evaluation of <sup>68</sup>Ga-labelled Cetuximab [<sup>68</sup>Ga]-**8** was carried out in EGFR expressing A431 xenograft-bearing mice. We first performed biodistribution and PET

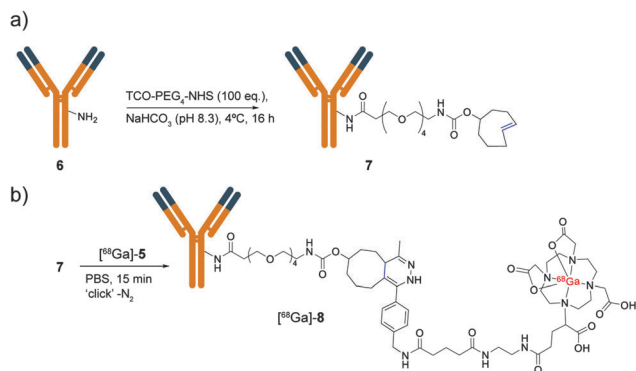


Fig. 2 (a) Synthesis of TCO-modified Cetuximab 7 and (b) radiolabelling via the IeDDA reaction with [<sup>68</sup>Ga]-5 to form dihydropyrazine [<sup>68</sup>Ga]-8.

imaging studies with either <sup>68</sup>GaCl<sub>3</sub> or [<sup>68</sup>Ga]-5 to investigate their corresponding pharmacokinetic profiles. <sup>68</sup>GaCl<sub>3</sub> accumulated in plasma and peripheral tissues, notably in relation to the small size of the tracer, resulting in overall high background activity (Fig. S4a and S5, ESI†). [<sup>68</sup>Ga]-5 was characterised by a rapid tissue distribution and subsequent clearance through the urinary route, yielding a low overall background activity (Fig. S4b and S6, ESI†). Neither <sup>68</sup>GaCl<sub>3</sub> nor [<sup>68</sup>Ga]-5 achieved significant accumulation in the tumour (Fig. 3; Fig. S4, S6 and S7, ESI†). We then performed PET studies where [<sup>68</sup>Ga]-8 was injected into animals and allowed to distribute for 3 h, followed by 60 min PET imaging; this showed sustained retention of the tracer and significant tumour detection (3.34 %ID mL<sup>-1</sup> at 60 min, compared to 0.60 %ID mL<sup>-1</sup> for [<sup>68</sup>Ga]-5, Fig. 3 and Fig. S7, ESI†). As anticipated, the PET image analysis also indicated a high retention of the activity in the liver, which is characteristic of the pharmacokinetic profile of a mAb (Fig. S6, ESI†).

We further assessed an *in vivo* pretargeting strategy, where the delivery of a radionuclide is separated from that of the mAb, and has the anticipated advantage of allowing for the TCO-modified Cetuximab to achieve optimal tumour accumulation and sufficient blood and non-tumour tissue clearance, before administration

of the radiolabelled reactive small molecule [<sup>68</sup>Ga]-5.<sup>1</sup> Cell uptake studies were performed using high (A431) and low (HCT116) EGFR-expressing cells, showing a significant and concentration-dependent activity retention in A431 cells pre-incubated with the TCO-modified Cetuximab 7, followed by incubation with [<sup>68</sup>Ga]-5 (Fig. S8, ESI†). Pre-incubation with non-modified Cetuximab 6 neutralised cell activity retention, and overall no detectable activity above background was found in HCT116 cells, highlighting the specificity and sensitivity of the pretargeting strategy. These data were comparable to the direct labelling setting with [<sup>68</sup>Ga]-8 (Fig. S8, ESI†). We then performed *in vivo* PET imaging in A431-xenograft bearing mice, where the animals were pre-treated with TCO-modified Cetuximab 7 for 3 or 23 h, followed by injection of ~1.85 MBq of [<sup>68</sup>Ga]-5. The PET image analysis indicated high retention of the activity in the liver, which is consistent with the characteristic pharmacokinetic profile of a mAb (Fig. S6, ESI†). Monoclonal antibodies, while having high affinity for targets of interest, also have inherently slow pharmacokinetics with high initial delivery to liver. The pretargeting strategy aims at conducting imaging studies when background distribution of the macromolecule in non-tumour tissue has decreased sufficiently to permit tumour-specific contrast. This aim is achieved in the 23 h protocol compared to the 3 h protocol. The PET images and derived data indicated no tumour detection with the 3 h treatment protocol, most probably attributed to the high concentration of antibody present in circulation at this time point, leading to the subsequent quenching of the injected [<sup>68</sup>Ga]-5 in circulation and possibly lower concentration of the antibody at the tumour site, consequently tumour radioactivity was lower in the 3 h compared to 23 h treatment protocol (0.86 %ID mL<sup>-1</sup> and 3.48 %ID mL<sup>-1</sup> at 60 min, respectively, Fig. 3; Fig. S6 and S7, ESI†). Moreover, we showed the significant superiority of the pretargeting approach over the traditional direct labelling method, through the analysis of the tumour to liver ratio, indicating a key high tumour to background signal when using the 1-day pretargeting protocol (T/L ratio 2.64, Fig. 3). It was noted that tumour uptake of <sup>68</sup>GaCl<sub>3</sub> (from γ-counting) was 5 %ID g<sup>-1</sup> compared to that of [<sup>68</sup>Ga]-5 and pretargeting at 1.8 and 3.34 %ID mL<sup>-1</sup>, respectively. While the time points of measurement are different, this observation initially questions the specificity of the pretargeting strategy. <sup>68</sup>GaCl<sub>3</sub> is a small molecule and its associated high non-specific uptake in some tumours has been reported, although the mechanism is not entirely clear.<sup>20</sup> In our study, this high uptake is only relevant if the metal is rapidly eliminated from the [<sup>68</sup>Ga]-5-complex. However, tumour uptake of [<sup>68</sup>Ga]-5 was found to be low precluding this possibility. The higher tumour uptake of radioactivity with the pretargeting strategy, compared to [<sup>68</sup>Ga]-5, therefore infers specific localisation.

In summary, we have developed a rapid and efficient method for the <sup>68</sup>Ga-labelling of a clinically relevant mAb, using the IeDDA reaction, and in high radiochemical yield. This represents a mild and efficient strategy for radiometal incorporation when compared to existing methods, which rely on direct labelling of mAbs containing functional chelates. We have demonstrated the utility of the labelling strategy through *in vivo* application for non-invasive PET imaging of EGFR, highlighting the potential utility

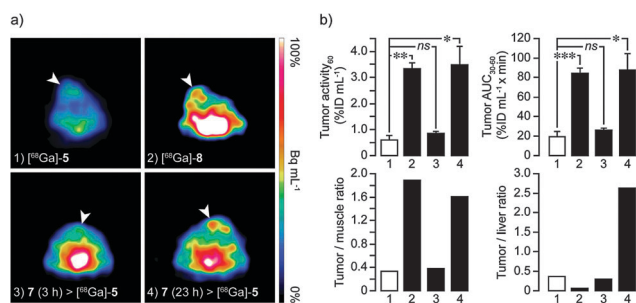


Fig. 3 'Direct' and 'pretargeted' PET imaging of EGFR-expressing A431 tumours. (a) Representative axial PET images of animal injected with [<sup>68</sup>Ga]-5 (*n* = 3), [<sup>68</sup>Ga]-8 (*n* = 5), TCO-modified Cetuximab 7 for 3 or 23 h followed by [<sup>68</sup>Ga]-5 ('pretargeting', *n* = 3 and 6, respectively). All scans were 60 min dynamic acquisition following a bolus injection of ~1.85 MBq of activity. The white arrowheads indicate the tumours. (b) PET extracted variables are shown: normalised tumour uptake at 60 min, area under the tumour TAC from 30 to 60 min.

of this conjugation method within a two-step pretargeting strategy. Future studies will investigate the application of this mAb bioorthogonal labelling conjugation approach for the annotation of various cell surface markers of cancer.

## Notes and references

- 1 L. Carroll, H. L. Evans, E. O. Aboagye and A. C. Spivey, *Org. Biomol. Chem.*, 2013, **11**, 5772–5781.
- 2 M. F. Debets, J. C. M. van Hest and F. P. J. T. Rutjes, *Org. Biomol. Chem.*, 2013, **11**, 6439–6455.
- 3 J. M. Baskin and C. R. Bertozzi, *QSAR Comb. Sci.*, 2007, **26**, 1211–1219.
- 4 J. A. Prescher, D. H. Dube and C. R. Bertozzi, *Nature*, 2004, **430**, 873–877.
- 5 H. L. Evans, R. L. Slade, L. Carroll, G. Smith, Q.-D. Nguyen, L. Iddon, N. Kamaly, H. Stockmann, F. J. Leeper, E. O. Aboagye and A. C. Spivey, *Chem. Commun.*, 2012, **48**, 991–993.
- 6 M. L. Blackman, M. Royzen and J. M. Fox, *J. Am. Chem. Soc.*, 2008, **130**, 13518–13519.
- 7 N. K. Devaraj and R. Weissleder, *Acc. Chem. Res.*, 2011, **44**, 816–827.
- 8 R. Rossin, S. M. van den Bosch, W. Ten Hoeve, M. Carvelli, R. M. Versteegen, J. Lub and M. S. Robillard, *Bioconjugate Chem.*, 2013, 1210–1217.
- 9 B. M. Zeglis, K. K. Sevak, T. Reiner, P. Mohindra, S. D. Carlin, P. Zanzonico, R. Weissleder and J. S. Lewis, *J. Nucl. Med.*, 2013, **54**, 1389–1396.
- 10 H. L. Evans, L. Carroll, E. O. Aboagye and A. C. Spivey, *J. Labelled Compd. Radiopharm.*, 2013, 219–297.
- 11 E. B. Corcoran and R. N. Hanson, *Med. Res. Rev.*, 2014, **34**, 596–643.
- 12 Y. Humblet, *Expert Opin. Pharmacother.*, 2004, **5**, 1621–1633.
- 13 H. J. Aerts, L. Dubois, L. Perk, P. Vermaelen, G. A. van Dongen, B. G. Wouters and P. Lambin, *J. Nucl. Med.*, 2009, **50**, 123–131.
- 14 W. Cai, K. Chen, L. He, Q. Cao, A. Koong and X. Chen, *Eur. J. Nucl. Med. Mol. Imaging*, 2007, **34**, 850–858.
- 15 W. Ping Li, L. A. Meyer, D. A. Capretto, C. D. Sherman and C. J. Anderson, *Cancer Biother. Radiopharm.*, 2008, **23**, 158–171.
- 16 D. Zeng, Y. Guo, A. G. White, Z. Cai, J. Modi, R. Ferdani and C. J. Anderson, *Mol. Pharmaceutics*, 2014, DOI: 10.1021/mp500004m.
- 17 M. R. Karver, R. Weissleder and S. A. Hilderbrand, *Bioconjugate Chem.*, 2011, **22**, 2263–2270.
- 18 J. Yang, M. R. Karver, W. Li, S. Sahu and N. K. Devaraj, *Angew. Chem., Int. Ed.*, 2012, **51**, 5222–5225.
- 19 N. K. Devaraj, R. Upadhyay, J. B. Haun, S. A. Hilderbrand and R. Weissleder, *Angew. Chem., Int. Ed.*, 2009, **48**, 7013–7016.
- 20 T. Ujula, S. Salomäki, A. Autio, P. Luoto, T. Tolvanen, P. Lehtikoinen, T. Viljanen, H. Sipilä, P. Härkönen and A. Roivainen, *Mol. Imaging Biol.*, 2010, **12**, 259–268.